

Characterization of the transcriptome, nucleotide sequence polymorphism, and natural selection in the desert adapted mouse *Peromyscus eremicus*

As a direct result of intense heat and aridity, deserts are thought to be among the most harsh of environments, particularly for their mammalian inhabitants. Given that osmoregulation can be challenging for these animals, with failure resulting in death, strong selection should be observed on genes related to the maintenance of water and solute balance. One such animal, *Peromyscus eremicus*, is native to the desert regions of the southwest United States and may live its entire life without oral fluid intake. As a first step toward understanding the genetics that underlie this phenotype, we present a characterization of the *P. eremicus* transcriptome. We assay four tissues (kidney, liver, brain, testes) from a single individual and supplement this with population level renal transcriptome sequencing from 15 additional animals. We identified a set of transcripts undergoing both purifying and balancing selection based on estimates of Tajima's D. In addition, we used the branch-site test to identify a transcript - *Slc2a9*, likely related to desert osmoregulation - undergoing enhanced selection in *P. eremicus* relative to a set of related non-desert rodents.

Characterization of the transcriptome, nucleotide sequence polymorphism, and natural selection in the desert adapted mouse *Peromyscus eremicus*

Matthew D. MacManes¹, Michael B. Eisen²,

¹ Department of Molecular, Cellular and Biomedical Sciences, University of New Hampshire, Durham NH, USA

² HHMI and University of California, Berkeley, Berkeley, CA, USA

* E-mail: macmanes@gmail.com, @PeroMHC

1 Abstract

2 As a direct result of intense heat and aridity, deserts are thought to be among the most harsh of
3 environments, particularly for their mammalian inhabitants. Given that osmoregulation can be
4 challenging for these animals, with failure resulting in death, strong selection should be observed
5 on genes related to the maintenance of water and solute balance. One such animal, *Peromyscus*
6 *eremicus*, is native to the desert regions of the southwest United States and may live its entire
7 life without oral fluid intake. As a first step toward understanding the genetics that underlie
8 this phenotype, we present a characterization of the *P. eremicus* transcriptome. We assay four
9 tissues (kidney, liver, brain, testes) from a single individual and supplement this with popu-
10 lation level renal transcriptome sequencing from 15 additional animals. We identified a set of
11 transcripts undergoing both purifying and balancing selection based on estimates of Tajima's
12 D. In addition, we used the branch-site test to identify a transcript -Slc2a9, likely related to
13 desert osmoregulation – undergoing enhanced selection in *P. eremicus* relative to a set of related
14 non-desert rodents.

15

16 Introduction

17 Deserts are widely considered one of the harshest environments on Earth. Animals living in
18 desert environments are forced to endure intense heat and drought, and as a result, species liv-
19 ing in these environments are likely to possess specialized mechanisms to deal with them. While
20 living in deserts likely involves a large number of adaptive traits, the ability to osmoregulate –
21 to maintain the proper water and electrolyte balance – appears to be paramount [1]. Indeed,
22 the maintenance of water balance is one of the most important physiologic processes for all
23 organisms, whether they be desert inhabitants or not. Most animals are exquisitely sensitive
24 to changes in osmolality, with slight derangement eliciting physiologic compromise. When the
25 loss of water exceeds dietary intake, dehydration - and in extreme cases, death - can occur.

26 Thus there has likely been strong selection for mechanisms supporting optimal osmoregulation
27 in species that live where water is limited. Understanding these mechanisms will significantly
28 enhance our understanding of the physiologic processes underlying osmoregulation in extreme
29 environments, which will have implications for studies of human health, conservation, and cli-
30 mate change.

31

32 The genes and structures responsible for the maintenance of water and electrolyte balance
33 are well characterized in model organisms such as mice [2], rats [3–5], and humans [6–8]. These
34 studies, many of which have been enabled by newer sequencing technologies, provide a founda-
35 tion for studies of renal genomics in non-model organisms. Because researchers have long been
36 interested in desert adaptation, a number of studies have looked at the morphology or expression
37 of single genes in the renal tissues of desert adapted rodents *Phyllotis darwini* [9], *Psammomys*
38 *obesus* [10], and *Perognathus penicillatus* [11]. More recently, full renal transcriptomes have
39 been generated for *Dipodomys spectabilis* and *Chaetodipus baileyi*, [12] as well as *Abrothrix oli-*
40 *vacea* [13].

41

42 These studies provide a rich context for current and future work aimed at developing a syn-
43 thetic understanding of the genetic and genomic underpinnings of desert adaptation in rodents.
44 As a first step, we have sequenced, assembled, and characterized the transcriptome (using four
45 tissue types - liver, kidney, testes and brain) of a desert adapted cricetid rodent endemic to the
46 southwest United States [14], *Peromyscus eremicus*. These animals have a lifespan typical of
47 small mammals, and therefore an individual may live its entire life without ever drinking water.
48 These rodents have distinct advantage over other desert animals (e.g. *Dipodomys*) in that they
49 breed readily in captivity, which enables future laboratory studies of the phenotype of interest.
50 In addition, the focal species is positioned in a clade of well known animals (e.g. *P. californicus*,
51 *P. maniculatus*, and *P. polionotus*) [15] with growing genetic and genomic resources [16–18].
52 Together, this suggests that future comparative studies are possible.

53

54 While the elucidation of the mechanisms underlying adaptation to desert survival is beyond
55 the scope of this manuscript, we aim to lay the groundwork by characterizing the transcriptome
56 from four distinct tissues (brain, liver, kidney, testes). These data will be included in the current
57 larger effort aimed at sequencing the entire genome. Further, via sequencing the renal tissue
58 of a total of 15 additional animals, we characterize nucleotide polymorphism and genome-wide
59 patterns of natural selection. Together, these investigations will aid in our overarching goal to
60 understand the genetic basis of adaptation to deserts in *P. eremicus*.

61 **Materials and Methods**

62 **Animal Collection and Study Design**

63 To begin to understand how genes may underlie desert adaptation, we collected 16 individuals
64 from a single population of *P. eremicus* over a two-year time period (2012-2013). These individ-
65 uals were captured in live traps and then euthanized using isoflurane overdose and decapitation.
66 Immediately post-mortem, the abdominal and pelvic organs were removed, cut in half (in the
67 case of the kidneys), placed in RNAlater and flash frozen in liquid Nitrogen. Removal of the
68 brain, with similar preservation techniques, followed. Time from euthanasia to removal of all
69 organs never exceeded five minutes. Samples were transferred to a -80C freezer at a later date.
70 These procedures were approved by the Animal Care and Use Committee located at the Univer-
71 sity of California Berkeley (protocol number R224) and University of New Hampshire (protocol
72 number 130902) as well as the California Department of Fish and Game (protocol SC-008135)
73 and followed guidelines established by the American Society of Mammalogy for the use of wild
74 animals in research [19].

75 **RNA extraction and Sequencing**

76 Total RNA was extracted from each tissue using a TRIzol extraction (Invitrogen) following the
77 manufacturer's instructions. Because preparation of an RNA library suitable for sequencing is
78 dependent on having high quality, intact RNA, a small aliquot of each total RNA extract was
79 analyzed on a Bioanalyzer 2100 (Agilent, Palo Alto, CA, USA). Following confirmation of sample
80 quality, the reference sequencing libraries were made using the TruSeq stranded RNA prep kit
81 (Illumina), while an unstranded TruSeq kit was used to construct the other sequencing libraries.
82 A unique index was ligated to each sample to allow for multiplexed sequencing. Reference
83 libraries (n=4 tissue types) were then pooled to contain equimolar quantities of each individual
84 library and submitted for Illumina sequencing using two lanes of 150nt paired end sequencing
85 employing the rapid-mode of the HiSeq 2500 sequencer at The Hubbard Center for Genome
86 Sciences (University of New Hampshire). The remaining 15 libraries were similarly multiplexed
87 and sequenced in a mixture of 100nt paired and single end sequencing runs across several lanes
88 of an Illumina HiSeq 2000 at the Vincent G. Coates Genome Center (University of California,
89 Berkeley).

90 **Sequence Data Preprocessing and Assembly**

91 The raw sequence reads corresponding to the four tissue types were error corrected using the
92 software `bless` version 0.17 [20] using `kmer=25`, based on the developer's default recommenda-
93 tions. The error-corrected sequence reads were adapter and quality trimmed following recom-

194 mendations from MacManes [21] and Mbandi [22]. Specifically, adapter sequence contamination
195 and low quality nucleotides (defined as PHRED <2) were removed using the program Trim-
196 momatic version 0.32 [23]. Reads from each tissue were assembled using the Trinity version
197 released 17 July 2014 [24]. We used flags to indicate the stranded nature of sequencing reads
198 and set the maximum allowable physical distance between read pairs to 999nt. The assembly
199 was conducted on a linux workstation with 64 cores and 512Gb RAM. To filter the raw se-
200 quence assembly, we downloaded *Mus musculus* cDNA and ncRNA datasets from Ensembl ([ftp:](ftp://ftp.ensembl.org/pub/release-75/fasta/mus_musculus/)
201 [//ftp.ensembl.org/pub/release-75/fasta/mus_musculus/](ftp://ftp.ensembl.org/pub/release-75/fasta/mus_musculus/)) and the *Peromyscus manica-*
202 *tus* reference transcriptome from NCBI ([ftp://ftp.ncbi.nlm.nih.gov/genomes/Peromyscus_](ftp://ftp.ncbi.nlm.nih.gov/genomes/Peromyscus_maniculatus_bairdii/RNA/)
203 [maniculatus_bairdii/RNA/](ftp://ftp.ncbi.nlm.nih.gov/genomes/Peromyscus_maniculatus_bairdii/RNA/)). We used a blastN (version 2.2.29+) procedure (default settings,
204 evaluate set to 10^{-10}) to identify contigs in the *P. eremicus* dataset likely to be biological in origin.
205 This procedure, when a reference dataset is available, retains more putative transcripts than a
206 strategy employing expression-based filtering (remove if TMP <1 [25]) of the raw assembly. We
207 then concatenated the filtered assemblies from each tissue into a single file and reduced redun-
208 dancy using the software cd-hit-est version 4.6 [26] using default setting, except that sequences
209 were clustered based on 95% sequence similarity. This multi-fasta file was used for all subsequent
210 analyses, including annotation and mapping.

211

212 **Assembled Sequence Annotation**

213 The filtered assemblies were annotated using the default settings of the blastN algorithm [27]
214 against the Ensembl cDNA and ncRNA datasets described above, downloaded on 1 August
215 2014. Among other things, the Ensemble transcript identifiers were used in the analysis of
216 gene ontology conducted in the PANTHER package [28]. Next, because rapidly evolving nu-
217 cleotide sequences may evade detection by blast algorithms, we used HMMER3 version 3.1b1 [29]
218 to search for conserved protein domains contained in the dataset using the Pfam database
219 [30]. Lastly, we extracted putative coding sequences using Transdecoder version 4Jul2014
220 (<http://transdecoder.sourceforge.net/>)

221

222 To identify patterns of gene expression unique to each tissue type, we mapped sequence reads
223 from each tissue type to the reference assembly using bwa-mem (version cloned from Github
224 7/1/2014) [31]. We estimated expression for the four tissues individually using default settings
225 of the software eXpress version 1.51 [32]. Interesting patterns of expression, including instances
226 where expression was limited to a single tissue type, were identified and visualized.

227

128 Population Genomics

129 In addition to the reference individual sequenced at four different tissue types, we sequenced
130 15 other conspecific individuals from the same population in Palm Desert, California. Sequence
131 data were mapped to the reference transcriptome using bwa-mem. The alignments were sorted
132 and converted to BAM format, then passed to the program ANGSD version 0.610, which was
133 used for calculating the folded site frequency spectrum (SFS) and Tajima's D [33].

134

135 Natural Selection

136 To characterize natural selection on several genes related to water and ion homeostasis, we iden-
137 tified several of the transcripts identified as experiencing positive selection in a recent work on
138 desert-adapted *Dipodomys* rodents. The coding sequences corresponding to these genes, Solute
139 Carrier family 2 member 9 (Slc2a9) and the Vitamin D3 receptor (Vdr), were extracted from
140 the dataset, aligned using the software MACSE version 1.01b [34] to homologous sequences in
141 *Mus musculus*, *Rattus norvegicus*, *Peromyscus maniculatus*, and *Homo sapiens* as identified by
142 the conditional reciprocal best blast procedure (CRBB, [35]). An unrooted gene tree was con-
143 structed using the online resource Clustal-Omega, and the tree and alignment were analyzed
144 using the branch-site model (model=2, nsSites=2, fix_omega=0 versus model=2, nsSites=2,
145 fix_omega=1, omega=1) implemented in PAML version 4.8 [36,37]. Significance was evaluated
146 via the use of the likelihood ratio test.

147

148 Results and Discussion

149 RNA extraction, Sequencing, Assembly, Mapping

150 RNA was extracted from the hypothalamus, renal medulla, testes, and liver from each individual
151 using sterile technique. TRIzol extraction resulted in a large amount of high quality (RIN \geq
152 8) total RNA, which was then used as input. Libraries were constructed as per the standard
153 Illumina protocol and sequenced as described above. The number of reads per library varied
154 from 56 million strand-specific paired-end reads in Peer360 kidney, to 9 million single-end reads
155 in Peer321 (Table 1, available on the Short Read Archive accession XXX). Adapter sequence
156 contamination and low-quality nucleotides were eliminated, which resulted in a loss of $<2\%$ of
157 the total number of reads. These trimmed reads served as input for all downstream analyses.

158 Table 1

159

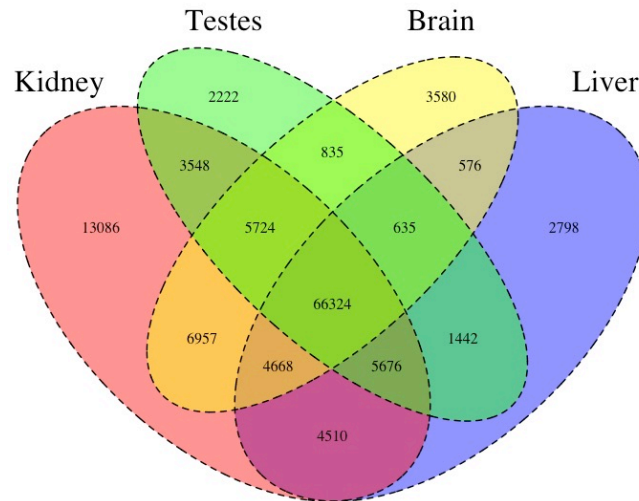
DATASET	NUM. RAW READS
PEER360 TESTES	32M PE/SS
PEER360 LIVER	53M PE /SS
PEER360 KIDNEY	56M PE/SS
PEER360 BRAIN	23M PE/SS
PEER305	19M PE
PEER308	15M PE
PEER319	14M PE
PEER321	9M SE
PEER340	16M PE
PEER352	14M PE
PEER354	9M SE
PEER359	14M PE
PEER365	16M PE
PEER366	16M PE
PEER368	14M PE
PEER369	14M PE
PEER372	17M SE
PEER373	23M SE
PEER380	16M SE
PEER382	14M SE

160

161 Table 1. The number of sequencing reads per sample, indicated by Peer[number]. PE=paired
 162 end, SS=strand specific, SE=single end sequencing.

163 Transcriptome assembly for each tissue type was accomplished using the program Trin-
 164 ity [24]. The raw assembly for brain, liver, testes, and kidney contained 185425, 222096, 180233,
 165 and 514091 assembled sequences respectively. This assembly was filtered using a blastN pro-
 166 cedure against the *Mus* cDNA and ncRNA and *P. maniculatus* cDNAs, which resulted in a
 167 final dataset containing 68331 brain-specific transcripts, 71041 liver-specific transcripts, 67340
 168 testes-specific transcripts, and 113050 kidney-specific transcripts. Mapping the error-corrected
 169 adapter/quality trimmed reads to these datasets resulted in mapping 94.98% (87.01% properly
 170 paired) of the brain-derived reads to the brain transcriptome, 96.07% (88.13% properly paired)
 171 of the liver-derived reads to the liver transcriptome, 96.81% (85.10% properly paired) of the
 172 testes-derived reads to the testes transcriptome, and 91.87% (83.77% properly paired) of the
 173 kidney-derived reads to the kidney transcriptome. Together, these statistics suggest that the
 174 tissue-specific transcriptomes are of extremely high quality. All tissue-specific assemblies are to
 175 be made available on Dryad.

176

177 **Figure 1**

178

179 Figure 1. The Venn Diagram.

180 We then estimated gene expression on each of these tissue-specific datasets, which allowed
 181 us to understand expression patterns in the multiple tissues. Specifically, we constructed a Venn
 182 diagram (Figure 1) that allowed us to visualize the proportion of genes whose expression was
 183 limited to a single tissue and those whose expression was ubiquitous. 66324 transcripts are
 184 expressed on all tissue types, while 13086 are uniquely expressed in the kidney, 2222 in the
 185 testes, 3580 in the brain, and 2798 in the liver. The kidney appears to an outlier in the number
 186 of unique sequences, though this could be the result of the recovery of more lowly expressed
 187 transcripts that may be the result of deeper sequencing.

188

189 In addition to this, we estimated mean TMP (number of transcripts per million) for all tran-
 190 scripts. Table 2 consists of the 10 genes whose mean TMP was the highest. Several genes in this
 191 list are predominately present in a single tissue type. For instance Transcript_126459, Albumin
 192 is very highly expressed in the liver, but less so in the other tissues. It should be noted, however,
 193 that making inference based on uncorrected values for TPM is not warranted. Statistical testing
 194 for differential expression was not implemented due to the fact that no replicates are available.

195

196 After expression estimation, the filtered assemblies were concatenated together, and after
 197 the removal of redundancy with cd-hit-est, 123,123 putative transcripts remained (to be made

available on Genbank). From this filtered concatenated dataset, we extracted 71626 putative coding sequences (72Mb, to be made available on Dryad). Of these 71626 sequences, 38221 were complete exons (containing both start and stop codons), while the others were either truncated at the 5-prime end (20239 sequences), the 3-prime end (6445 sequences), or were internal (6721 sequencing with neither stop nor start codon). The results of a Pfam search conducted on the predicted amino acid sequences will be found on Dryad.

Table 2

Transcript ID	Testes	Liver	Kidney	Brain	Genbank ID	Gene ID
Transcript_83842	2.05E+03	6.40E+03	1.03E+04	5.47E+03	DQ073446.1	COX2
Transcript_126459	1.43E+01	2.22E+04	2.77E+01	6.73E+00	XM_006991665.1	Alb
Transcript_128937	4.39E+00	1.91E+04	4.74E+02	2.23E+00	XM_007627625.1	Apoa2
Transcript_81233	1.71E+03	5.23E+03	6.11E+03	3.08E+03	XM_006993867.1	Fth1
Transcript_94125	3.67E+01	1.08E+04	2.09E+03	2.75E+00	XM_006977178.1	CytP450
Transcript_119945	5.03E+03	1.15E+03	1.33E+03	3.71E+03	XM_008686011.1	Ubb
Transcript_5977	4.95E+00	1.01E+04	3.05E+02	3.58E+02	XM_006978668.1	Tf
Transcript_4057	2.62E+01	9.32E+03	1.34E+02	8.38E+01	XM_006994871.1	Apoc1
Transcript_112523	4.07E+02	7.36E+03	7.78E+02	9.54E+02	XM_006994872.1	Apoe
Transcript_98376	1.98E+00	8.66E+03	1.02E+00	2.68E+00	XM_006970208.1	Ttr

Table 2. The 10 transcripts with the highest mean TPM (transcripts per million).

Population Genomics

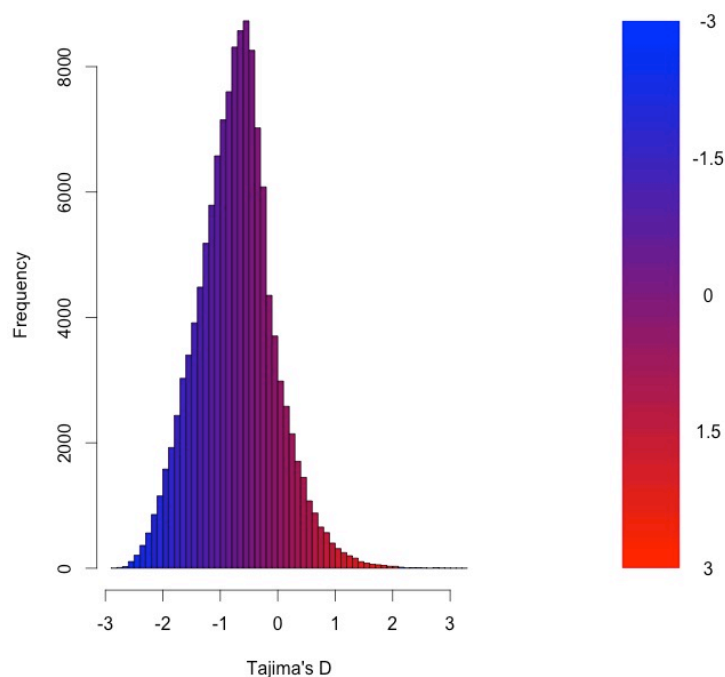
As detailed above, RNAseq data from 15 individuals were mapped to the reference transcriptome with the resulting BAM files being used as input to the software package ANGSD. The Tajima's D statistic was calculated for all transcripts covered by at least 14 of the 15 individuals. In brief, a negative Tajima's D - a result of lower than expected average heterozygosity - is often associated with purifying or directional selection, recent selective sweep or population bottleneck. In contrast, a positive value for Tajima's D represents higher than expected average heterozygosity, often associated with balancing selection.

The distribution of the estimates of Tajima's D for all of the assembled transcripts is shown in Figure 2. The distribution is skewed toward negative values (mean=-0.89, variance=0.58), which is likely the result of purifying selection, a model of evolution commonly invoked for coding DNA sequences [38]. Table 3 presents the 10 transcripts whose estimate of Tajima's D is the greatest, while Table 4 presents the 10 transcripts whose estimate of Tajima's D is the

223 least. The former list of genes is likely to contain transcripts experiencing balancing selection
224 in the studied population. This list includes, interestingly, genes obviously related to solute
225 and water balance (e.g. *Clnkb* and a transmembrane protein gene) and immune function (a
226 interferon-inducible GTPase and a Class 1 MHC gene). The latter group, containing transcripts
227 whose estimates of Tajima's D are the smallest are likely experiencing purifying selection. Many
228 of these transcripts are involved in core regulatory functions where mutation may have strongly
229 negative fitness consequences.

230

231 **Figure 2**



232

233 Figure 2. The distribution of Tajima's D for all putative transcripts.

234 **Table 3**

235

Transcript ID	GenBank ID	Description	Tajima's D
Transcript_49049	XM_006533884.1	heterogeneous nuclear ribonucleoprotein H1 (Hnrnp1)	3.26
Transcript_38378	XM_006522973.1	Son DNA binding protein (Son)	3.19
Transcript_126187	NM_133739.2	transmembrane protein 123 (Tmem123)	3.02
Transcript_70953	XM_006539066.1	chloride channel Kb (Clcnkb)	2.96
Transcript_37736	XM_006997718.1	h-2 class I histocompatibility antigen	2.92
Transcript_21448	XM_006986148.1	zinc finger protein 624-like	2.84
Transcript_47450	NM_009560.2	zinc finger protein 60 (Zfp60)	2.82
Transcript_122250	XM_006539068.1	chloride channel Kb (Clcnkb)	2.81
Transcript_78367	XM_006496814.1	CDC42 binding protein kinase alpha (Cdc42bpa)	2.78
Transcript_96470	XM_006987129.1	interferon-inducible GTPase 1-like	2.77

Table 3. The 10 transcripts with the highest values for Tajima's D, which suggests balancing selection.

238 Table 4

239

Transcript ID	GenBank ID	Description	Tajima's D
Transcript_84359	XM_006991127.1	nuclear receptor coactivator 3 (Ncoa3)	-2.82
Transcript_87121	XM_006970128.1	methyl-CpG binding domain protein 2 (Mbd2)	-2.82
Transcript_125755	EU053203.1	alpha globin gene cluster	-2.78
Transcript_87128	XM_006976644.1	membrane-associated ring finger (March5)	-2.76
Transcript_55468	XM_006978377.1	Vpr binding protein (Vprbp)	-2.75
Transcript_116042	XM_006980811.1	membrane associated guanylate kinase (Magi3)	-2.75
Transcript_18966	XM_006982814.1	ubiquitin protein ligase E3 component n-recognin 5 (Ubr5)	-2.75
Transcript_122204	XM_008772511.1	zinc finger protein 612 (Zfp612)	-2.75
Transcript_100550	XM_006971297.1	bromodomain adjacent to zinc finger domain, 1B (Baz1b)	-2.74
Transcript_33267	XM_006975561.1	pumilio RNA-binding family member 1 (Pum1)	-2.75

Table 4. The 10 transcripts with the lowest values for Tajima's D, which suggests purifying or directional selection.

242 Natural Selection

243 To begin to test the hypothesis that selection on transcripts related to osmoregulation is en-
 244 hanced in the desert adapted *P. eremicus*, we implemented the branch-site test as described
 245 above by setting the sequence corresponding to *P. eremicus* for both Slc2a9 and Vdr as the
 246 foreground lineages in 2 distinct program executions. These two transcripts were chosen specifi-
 247 cally because they - the former significantly - were recently linked to osmoregulation in a desert

248 rodent [12]. The test for *Slc2a9* was highly significant ($2\Delta L_{nl}=51.4$, $df=1$, $p=0$), indicating en-
249 hanced selection in *P. eremicus* relative to the other lineages. The branch site test for positive
250 selection conducted on the *Vdr* gene was non-significant ($2\Delta L_{nl}=0.68$, $df=1$, $p=1$). This lim-
251 ited analysis of selection is to be followed up by an analysis of genome wide patterns of natural
252 selection.

253

254 Conclusions

255 As a direct result of intense heat and aridity, deserts are thought to be amongst the harshest
256 environments, particularly for mammalian inhabitants. Given that osmoregulation can be chal-
257 lenging for these animals - with failure resulting in death - strong selection should be observed on
258 genes related to the maintenance of water and solute balance. This study aimed to characterize
259 the transcriptome of a desert-adapted rodent species, *P. eremicus*. Specifically, we characterized
260 the transcriptome of four tissue types (liver, kidney, brain, and testes) from a single individual
261 and supplemented this with population-level renal transcriptome sequencing from 15 additional
262 animals. We identified a set of transcripts undergoing both purifying and balancing selection
263 based on Tajima's *D*. In addition, we used a branch site test to identify a transcript, likely
264 related to desert osmoregulation, undergoing enhanced selection in *P. eremicus* relative to a set
265 of non-desert rodents.

266

267 Acknowledgments

268 References

- 269 1. Walsberg G (2000) Small mammals in hot deserts: Some generalizations revisited. *Bio-*
270 *science* 50: 109–120.
- 271 2. Tatum R, Zhang Y, Salleng K, Lu Z, Lin JJ, et al. (2009) Renal salt wasting and chronic
272 dehydration in claudin-7-deficient mice. *Renal Physiology* 298: F24–F34.
- 273 3. Romero DG, Plonczynski MW, Welsh BL, Gomez-Sanchez CE, Zhou MY, et al. (2007)
274 Gene expression profile in rat adrenal zona glomerulosa cells stimulated with aldosterone
275 secretagogues. *Physiological Genomics* 32: 117–127.

- 276 4. Rojek A, Rojek A, Fuchtbauer E, Fuchtbauer E, Kwon T, et al. (2006) Severe urinary
277 concentrating defect in renal collecting duct-selective AQP2 conditional-knockout mice.
278 PNAS 103: 6037–6042.
- 279 5. Nielsen S, Chou C, Marples D, Christensen E, Kishore B, et al. (1995) Vasopressin
280 increases water permeability of kidney collecting duct by inducing translocation of
281 aquaporin-CD water channels to plasma-membrane. PNAS 92: 1013–1017.
- 282 6. Mobasheri A, Marples D, Young IS, Floyd RV, Moskaluk CA, et al. (2007) Distribution
283 of the AQP4 Water Channel in Normal Human Tissues: Protein and Tissue Microarrays
284 Reveal Expression in Several New Anatomical Locations, including the Prostate Gland
285 Seminal Vesicles. Channels 1: 30–39.
- 286 7. Bedford JJ, Leader JP, Walker RJ (2003) Aquaporin expression in normal human kidney
287 and in renal disease. Journal of the American Society of Nephrology 14: 2581–2587.
- 288 8. Nielsen S, Kwon TH, Christensen BM, Promeneur D, Frøkiaer J, et al. (1999) Physiology
289 and pathophysiology of renal aquaporins. Journal of the American Society of Nephrology
290 10: 647–663.
- 291 9. Gallardo PA, Cortés A, Bozinovic F (2005) Phenotypic flexibility at the molecular and
292 organismal level allows desert-dwelling rodents to cope with seasonal water availability.
293 Physiological and Biochemical Zoology 78: 145–152.
- 294 10. Kaissling B, De Rouffignac C, Barrett JM, Kriz W (1975) The structural organization
295 of the kidney of the desert rodent *Psammomys obesus*. Anatomy and Embryology 148:
296 121–143.
- 297 11. Altschuler EM, Nagle RB, Braun EJ, Lindstedt SL, Krutzsch PH (1979) Morphological
298 study of the desert heteromyid kidney with emphasis on the genus *Perognathus*. The
299 Anatomical Record 194: 461–468.
- 300 12. Marra NJ, Romero A, DeWoody JA (2014) Natural selection and the genetic basis of
301 osmoregulation in heteromyid rodents as revealed by RNA-seq. Molecular Ecology 23:
302 2699–2711.
- 303 13. Giorello FM, Feijoo M, D'Elía G, Valdez L, Opazo JC, et al. (2014) Characterization of
304 the kidney transcriptome of the South American olive mouse *Abrothrix olivacea*. BMC
305 Genomics 15: 446.
- 306 14. Veal R, Caire W (2001) *Peromyscus eremicus*. Mammalian Species 118: 1–6.

- 307 15. Feng BJ, Sun LD, Soltani-Arabshahi R, Bowcock AM, Nair RP, et al. (2007) Toward
308 a Molecular Phylogeny for *Peromyscus*: Evidence from Mitochondrial Cytochrome- b
309 Sequences. *Journal of Mammalogy* 88: 1146–1159.
- 310 16. Shorter KR, Owen A, anderson V, Hall-South AC, Hayford S, et al. (2014) Natural genetic
311 variation underlying differences in *Peromyscus* repetitive and social/aggressive behaviors.
312 *Behavior genetics* 44: 126–135.
- 313 17. Panhuis TM, Broitman-Maduro G, Uhrig J, Maduro M, Reznick DN (2011) Analysis of
314 Expressed Sequence Tags from the Placenta of the Live-Bearing Fish Poeciliopsis (Poe-
315 ciliidae). *Journal of Heredity* 102: 352–361.
- 316 18. Shorter KR, Crossland JP, Webb D, Szalai G, Felder MR, et al. (2012) *Peromyscus* as a
317 Mammalian Epigenetic Model. *Genetics Research International* 2012: 1–11.
- 318 19. Sikes RS, Gannon WL, Animal Care and Use Committee of the American Society of
319 Mammalogists (2011) Guidelines of the American Society of Mammalogists for the use of
320 wild mammals in research. *Journal of Mammalogy* 92: 235–253.
- 321 20. Heo Y, Wu XL, Chen D, Ma J, Hwu WM (2014) BLESS: Bloom filter-based error correc-
322 tion solution for high-throughput sequencing reads. *Bioinformatics* 30: 1354–1362.
- 323 21. MacManes MD (2014) On the optimal trimming of high-throughput mRNA sequence
324 data. *Frontiers in Genetics* 5.
- 325 22. Mbandi SK, Hesse U, Rees DJG, Christoffels A (2014) A glance at quality score: Impli-
326 cation for *de novo* transcriptome reconstruction of Illumina reads. *Frontiers in Genetics*
327 5: 17.
- 328 23. Lohse M, Bolger AM, Nagel A, Fernie AR, Lunn JE, et al. (2012) RobiNA: A user-friendly,
329 integrated software solution for RNA-Seq-based transcriptomics. *Nucleic Acids Research*
330 40: W622–7.
- 331 24. Haas BJ, Papanicolaou A, Yassour M, Grabherr M, Blood PD, et al. (2013) *De novo*
332 transcript sequence reconstruction from RNA-seq using the Trinity platform for reference
333 generation and analysis. *Nature Protocols* 8: 1494–1512.
- 334 25. **MacManes** MD, Lacey EA (2012) The Social Brain: Transcriptome Assembly and Char-
335 acterization of the Hippocampus from a Social Subterranean Rodent, the Colonial Tuco-
336 Tuco (*Ctenomys sociabilis*). *PLOS ONE* 7: e45524.

- 337 26. Li W, Godzik A (2006) Cd-hit: A fast program for clustering and comparing large sets of
338 protein or nucleotide sequences. *Bioinformatics* 22: 1658–1659.
- 339 27. Camacho C, Coulouris G, Avagyan V, Ma N, Papadopoulos J, et al. (2009) BLAST+:
340 architecture and applications. *BMC Bioinformatics* 10: 421.
- 341 28. Mi H (2004) The PANTHER database of protein families, subfamilies, functions and
342 pathways. *Nucleic Acids Research* 33: D284–D288.
- 343 29. Wheeler TJ, Eddy SR (2013) nhmmer: DNA homology search with profile HMMs. *Bioin-*
344 *formatics* 29: 2487–2489.
- 345 30. Punta M, Coggill PC, Eberhardt RY, Mistry J, Tate J, et al. (2012) The Pfam protein
346 families database. *Nucleic Acids Research* 40: D290–301.
- 347 31. Li H (2013) Aligning sequence reads, clone sequences and assembly contigs with BWA-
348 MEM. arXivorg .
- 349 32. Roberts A, Pachter L (2013) Streaming fragment assignment for real-time analysis of
350 sequencing experiments. *Nature Methods* 10: 71–73.
- 351 33. Korneliussen I Thorfinn Sand Moltke, Albrechtsen a, Nielsen R (2013) Calculation of
352 Tajima’s D and other neutrality test statistics from low depth next-generation sequencing
353 data. *BMC Bioinformatics* 14: 289.
- 354 34. Ranwez V, Harispe S, Delsuc F, Douzery EJP (2011) MACSE: Multiple Alignment of
355 Coding SEquences Accounting for Frameshifts and Stop Codons. *PLOS ONE* 6: e22594.
- 356 35. Aubry S, Kelly S, Kämpers BMC, Smith-Unna RD, Hibberd JM (2014) Deep Evolutionary
357 Comparison of Gene Expression Identifies Parallel Recruitment of Trans-Factors in Two
358 Independent Origins of C4 Photosynthesis. *PLOS Genetics* 10: e1004365.
- 359 36. Yang Z, dos Reis M (2011) Statistical Properties of the Branch-Site Test of Positive
360 Selection. *Molecular Biology and Evolution* 28: 1217–1228.
- 361 37. Yang Z (2007) PAML 4: Phylogenetic Analysis by Maximum Likelihood. *Molecular*
362 *Biology and Evolution* 24: 1586–1591.
- 363 38. Chamary JV, Parmley JL, Hurst LD (2006) Hearing silence: non-neutral evolution at
364 synonymous sites in mammals. *Nature Reviews Genetics* 7: 98–108.